

Study of radiation damage in Li_2O by means of electron-spin resonance

K. Noda, K. Uchida,* T. Tanifuji, and S. Nasu

Japan Atomic Energy Research Institute, Tokai-mura, Naka-gun, Ibaraki-ken, 319-11 Japan

(Received 19 June 1980; revised manuscript received 7 April 1981)

ESR spectra with a hyperfine structure consisting of more than 20 peaks were observed in Li_2O single crystals, irradiated by energetic tritons and helium ions formed by 6×10^{22} to 6×10^{25} ${}^6\text{Li}(n, \alpha)\text{-}{}^3\text{H}$ reactions per m^3 introduced with the order of 10^{20} to 10^{23} thermal neutrons per m^2 . The g value of the spectra was 2.002 ± 0.001 , and the hyperfine structure depended on the orientation of the specimens relative to the applied magnetic field. From the angular dependence the spectra were attributed to F^+ centers (an oxygen vacancy trapping an electron). In Li_2O single crystals irradiated to the order of 10^{23} thermal neutrons per m^2 , colloidal Li metal centers were not observed, in direct contrast with the situations in sintered Li_2O pellets. Isochronal and isothermal annealing experiments were done and the recovery behavior of the F^+ centers was observed. From the isothermal annealing experiments, the activation energy for recovery of the F^+ centers was determined to be about 135 kJ/mol (1.4 eV).

I. INTRODUCTION

Lithium oxide (Li_2O) has been selected as a solid-state blanket breeding material in the conceptual designs of a tokamak experimental fusion reactor, JXFR, at Japan Atomic Energy Research Institute¹ (JAERI) and a laser fusion reactor, SOLASE, at the University of Wisconsin.² The blanket material during operation of the fusion reactors will be attacked by the following three kinds of severe radiations: (1) neutrons with the kinetic energies up to 14.1 MeV; (2) tritons (2.7 MeV) and helium ions (2.1 MeV) produced by the ${}^6\text{Li}(n, \alpha)\text{-}{}^3\text{H}$ reactions, and (3) γ rays. These radiations will induce various kinds of radiation damage in Li_2O .

Radiation damage in crystals with the anticalcium fluoride structure such as Li_2O has scarcely been investigated, although studies of optical absorption³ (sintered pellets and single crystals) and ESR^{4,5} (pressed powder and sintered pellets) in neutron-irradiated Li_2O have been reported.

In this paper, a paramagnetic lattice defect, that is, the F^+ center, and its recovery behavior in neutron-irradiated Li_2O single crystals are investigated by the ESR method.

II. EXPERIMENTAL

A. Specimens

The specimens used were Li_2O single crystals and the preparation method was described in detail elsewhere.⁶ The starting material was Li_2O powder purchased from Cerac/Pure Co. Ltd. The powder was hydrostatically pressed into rods about 100 mm in

length and about 10 mm in diameter under pressure of 2×10^8 Pa and was sintered at 1370 K for 4 h in vacuum. From the sintered rods, the single crystals were grown in an argon atmosphere by the floating-zone melting technique using an infrared imaging furnace (Nichiden Machinery, Ltd., type SC-4). The single crystals were annealed at 1170 K for 2 h in vacuum, so that the strain induced by the large temperature gradient during crystal growth was removed. Chemical analysis of the single crystals was carried out by the extraction-photometry method, and the single crystals were confirmed to be zone refined in comparison with the starting powder. The typical impurities were as follows: Fe < 1 ppm, Al: 9 ppm, Ni < 1 ppm, Co < 1 ppm, and Cr < 1 ppm. The single crystals were cleaved on {111} planes or cut by a diamond cutter, to obtain specimens ($2 \times 2 \times 8$ mm³) having the rotational axis as the $\langle 110 \rangle$ direction.

B. Irradiation

Neutron irradiations were done in JRR-4 (low-neutron fluences) and JRR-2 (high-neutron fluences) at JAERI. In JRR-4, the thermal neutron flux and the fast neutron flux were $(3 \text{ to } 4) \times 10^{17}$ and $(4 \text{ to } 6) \times 10^{16}$ neutrons per m^2 sec, respectively, and the ratio of the thermal neutron flux to the epithermal neutron flux was about 45. In JRR-2, the thermal neutron flux and the fast neutron flux were 2.6×10^{17} and 1×10^{15} neutrons per m^2 sec, respectively. The thermal neutron fluences were measured by determining the γ activity of cobalt or cobalt-aluminum wire monitors placed near the specimens. In order to keep the temperature of the specimens as low as possible, they were sealed in quartz tubes containing

about 6×10^4 Pa helium gas, a good thermal conductor, and irradiated in the water-cooled irradiation holes. The temperature of specimens during irradiation was estimated to be less than 373 K from the results of the recovery experiment described later.

In a reactor, the specimens are simultaneously irradiated by γ rays as well as by neutrons. The γ -ray dose rate in the reactors used was of the order of 7 Ci/kg sec (1×10^8 R/h). In order to study the effect of γ -ray irradiation on defect production, γ -ray irradiation was done at room temperature by a ^{60}Co γ -ray source at JAERI. The dose rate in this experiment was about 3.6×10^{-2} Ci/kg sec (5×10^5 R/h).

C. Electron-spin resonance measurements

Electron-spin resonance (ESR) measurements were carried out at room temperature with a JEOL JES-PE-3X homodyne spectrometer working at approximately 9400 MHz, employing a TE_{011} cylindrical cavity. A Hitachi MES-4002 X-band spectrometer was also used to check the g value. Magnetic field measurements were checked with a proton resonance gaussmeter and a Hewlett-Packard frequency counter (HP-5246 L).

III. RESULTS AND DISCUSSION

A. Observed electron-spin-resonance spectra

Electron-spin-resonance spectra exhibiting hyperfine structure were observed at room temperature from Li_2O single crystals irradiated to the order of 10^{20} to 10^{23} thermal neutrons per m^2 . The hyperfine structure was found to be dependent upon the crystal orientation in the applied magnetic field H by rotating the specimen around the $\langle 110 \rangle$ axis. Typical examples of the observed spectra for the low-index directions are shown in Fig. 1 together with hyperfine-line-intensity ratios predicted for the F^+ center in Li_2O , which will be discussed later. Traces 1(a), 1(b), and 1(c) were obtained with the Li_2O single crystal oriented so that \bar{H} was along the $\langle 100 \rangle$, $\langle 110 \rangle$, and $\langle 111 \rangle$ axes, respectively. The g value of these spectra was determined to be 2.002 ± 0.001 . The separations between peaks were in the range of 9.2 to 9.5 G, and the individual linewidths were in the range of 4.6 to 4.8 G.

These spectra were not observed in specimens before neutron irradiation or in those irradiated by ^{60}Co γ rays up to 2.5×10^4 Ci/kg (10^8 R). This suggests that the photochemical process does not readily occur in Li_2O and that the spectrum is due to a defect produced by energetic tritons (2.7 MeV) and helium ions (2.1 MeV) of the $^6\text{Li}(n, \alpha)^3\text{H}$ reactions with

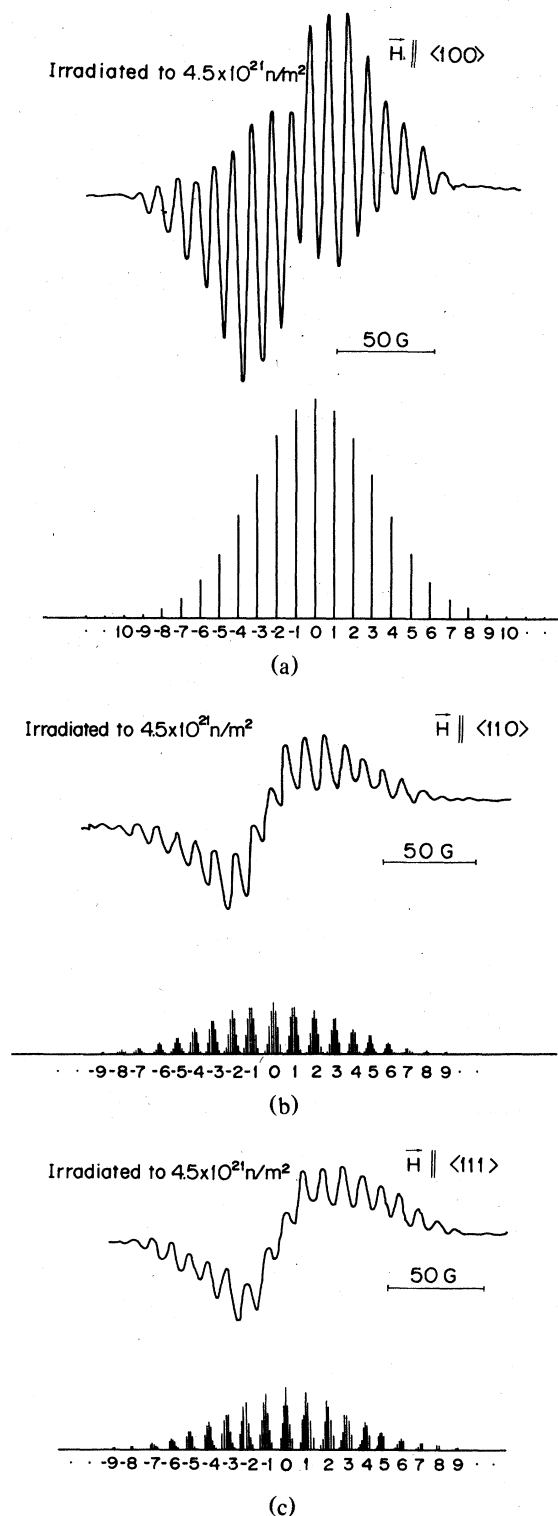


FIG. 1. (a)–(c) The ESR spectrum of the Li_2O single crystals irradiated to 4.5×10^{21} thermal neutrons per m^2 in the $\langle 100 \rangle$, $\langle 110 \rangle$, and $\langle 111 \rangle$ directions and the calculated relative intensity ratios of the hyperfine lines.

thermal neutrons (940 b for thermal neutron), or by fast neutrons. On the other hand, defect centers in the Li_2O single crystals irradiated in JRR-2 and JRR-4 have been studied by optical-absorption measurements.³ In that study, the formation of irradiation-induced damage in Li_2O was attributed to energetic tritons and helium ions produced by the ${}^6\text{Li}(n, \alpha){}^3\text{H}$ reactions by comparing the spectrum obtained by irradiation of neutrons cut off with Cd foils (only fast neutrons) with those obtained by irradiation without Cd foils (thermal and fast neutrons). From the above, the spectra in the present paper are attributed to the defect produced by energetic tritons and helium ions.

The electron-spin-resonance spectra were analyzed using the following equation assuming a F^+ center (oxygen-ion vacancy occupied by one electron) in Li_2O as shown in Fig. 2 and neglecting the nuclear Zeeman and nuclear quadrupole interaction energies:

$$h\nu_e = g\mu_B H_0 + \sum_{\gamma} M_{I\gamma} [a + b(3\cos^2\alpha_{\gamma} - 1)] \quad (1)$$

where each symbol has the usual meaning. The second term of Eq. (1) represents the hyperfine interaction between the electron of the F^+ center and the surrounding nuclei. The hyperfine coupling constants a and b indicate the isotropic interaction (i.e., Fermi contact term) and the anisotropic (dipole-dipole) interaction, respectively. α_{γ} is the angle between the direction of the applied magnetic field and the line joining the F^+ center with the neighboring Li nucleus. When n surrounding nuclei are equivalent, that is, the value of $[a + b(3\cos^2\alpha_{\gamma} - 1)]$ for each of n nuclei is equal, $M_{I\gamma}$ is represented by $M_{I\gamma} = nI, nI - 1, \dots, -nI + 1, -nI$, where I is the nuclear spin of the surrounding nuclei.

Li_2O has the anticalcium fluoride-type structure and each F^+ center is surrounded by 8 Li nuclei in the first shell and 12 O nuclei in the second shell. The natural abundance of oxygen nuclei with nuclear spin (${}^{17}\text{O}$) is 0.0373%, so that the oxygen nuclei have

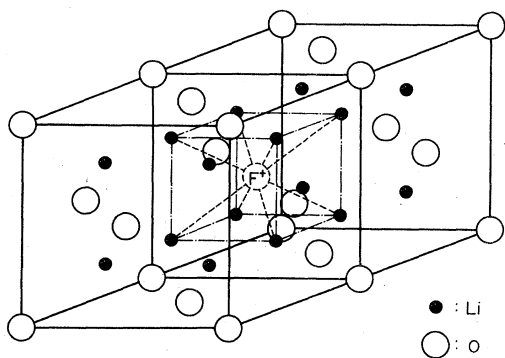


FIG. 2. A schematic illustration of the F^+ center in Li_2O .

little hyperfine interaction with the electron of the F^+ center. Furthermore, the hyperfine interaction due to Li nuclei beyond the second shell may be neglected, since their hyperfine coupling constants are assumed to be very small. Thus, only the hyperfine interaction with 8 Li nuclei in the first shell is taken into account for interpretation of the angular dependence of the ESR spectra.

Natural Li_2O contains about 92.6% ${}^7\text{Li}$ and about 7.4% ${}^6\text{Li}$. The probability $W(m)$ that the first shell of Li nuclei surrounding the F^+ centers contains m ${}^6\text{Li}$ nuclei and $(8 - m)$ ${}^7\text{Li}$ nuclei may be calculated by

$$W(m) = \binom{8}{m} (0.926)^{8-m} (0.074)^m \quad (2)$$

where the $\binom{8}{m}$ is the binominal coefficient. The probability for $m = 0, 1,$ and 2 is found to be 0.54, 0.35, and 0.10, respectively. ESR spectra for the F center in neutron-irradiated LiF single crystals enriched to 99.99% ${}^7\text{Li}$ were confirmed to be identical to those for LiF crystals with natural isotopic content, with respect to spacing and angular dependence of the resolved hyperfine lines, except that the resolution of the hyperfine lines was slightly improved for the former case.⁷ In LiF with natural isotopic content, the probability for zero, one, and two ${}^6\text{Li}$ nuclei appearing in the first shell is 0.63, 0.30, and 0.06, respectively. These probabilities are almost the same as that for Li_2O with natural isotopic content. This suggests that the effect of ${}^6\text{Li}$ nuclei on the hyperfine structure of the F^+ centers in Li_2O is small. Thus, all Li nuclei in the first shell of the F^+ centers in Li_2O with natural isotopic content can be assumed to be ${}^7\text{Li}$ with nuclear spin $I = \frac{3}{2}$ for simplicity.

Table I shows the values of α_{γ} in Eq. (1) and the number of nuclei belonging to the α_{γ} , when \vec{H} is parallel to the $\langle 100 \rangle$, $\langle 110 \rangle$, or $\langle 111 \rangle$ direction of the specimen. Applying the α_{γ} to Eq. (1) and rewriting Eq. (1) in terms of H at which the ESR absorp-

TABLE I. The angles α_{γ} and the number of Li nuclei belonging to the α_{γ} for the $\langle 100 \rangle$, $\langle 110 \rangle$, and $\langle 111 \rangle$ directions.

Orientation	α_{γ}	Number of Li nuclei
$\vec{H} \parallel \langle 100 \rangle$	$\alpha = 54.74^\circ$	8
$\vec{H} \parallel \langle 110 \rangle$	$\alpha_1 = 35.26^\circ$	4
	$\alpha_2 = 90.00^\circ$	4
$\vec{H} \parallel \langle 111 \rangle$	$\alpha_1 = 0^\circ$	2
	$\alpha_2 = 70.53^\circ$	6

tion may occur, the equations interpreting the ESR spectra in the $\langle 100 \rangle$, $\langle 110 \rangle$, and $\langle 111 \rangle$ directions are given by

$$H = H_0 + a' M_{I_1}, \quad \vec{H} \parallel \langle 100 \rangle, \quad (3)$$

$$H = H_0 + (a' + b') M_{I_1} + (a' - b') M_{I_2}, \quad \vec{H} \parallel \langle 110 \rangle, \quad (4)$$

$$H = H_0 + (a' + 2b') M_{I_1} + (a' - 0.67b') M_{I_2}, \quad \vec{H} \parallel \langle 111 \rangle, \quad (5)$$

where $a' = a/g\mu_B$, $b' = b/g\mu_B$, and M_{I_i} can take integer values ($-12 \leq M_{I_1} \leq 12$ for the $\langle 100 \rangle$, $-6 \leq M_{I_1}, M_{I_2} \leq 6$ for the $\langle 110 \rangle$, and $-3 \leq M_{I_1} \leq 3$, $-9 \leq M_{I_2} \leq 9$ for the $\langle 111 \rangle$ directions).

In the case of the $\langle 100 \rangle$ direction, the statistical weight ratios among the 25 levels of M_{I_1} are $M_{I_1}(12):M_{I_1}(11):\dots:M_{I_1}(0):\dots:M_{I_1}(-12) = 1:8:36:120:322:728:1428:2472:3823:5328:6728:7728:8092:7728:\dots:8:1$. According to Eq. (3), 25 lines of hyperfine structure are located at an interval of a' , and the relative intensity ratios of each hyperfine line are equal to the statistical weight ratios of M_{I_1} .

In the case of the $\langle 110 \rangle$ direction, the statistical weight ratios among each level of M_{I_1} and M_{I_2} are $M_{I_1}, M_{I_2}(6):M_{I_1}, M_{I_2}(5):\dots:M_{I_1}, M_{I_2}(-6) = 1:4:10:20:31:40:44:40:\dots:4:1$. A value of H corresponding to the position of the hyperfine line occurs for every combination of values of $(a' + b')M_{I_1}$ and $(a' - b')M_{I_2}$ being independent each other. The relative weight of the ESR transition occurring at a particular value of H is the product of the above-mentioned weights of M_{I_1} and M_{I_2} under consideration. In this manner, the relative intensity ratios are determined for $(13)^2$ or 169 hyperfine lines. The value of b is considered to be small in comparison with that of a , since the angular dependence of separation between peaks of the observed spectra was small and the number of peaks was unchanged for all directions. Consequently, 169 lines are segregated into 25 groups and the separation of each line in each group is $2b'$ G.

In the case of the $\langle 111 \rangle$ direction, the statistical weight ratios among levels of M_{I_1} and M_{I_2} are as follows; $M_{I_1}(3):M_{I_1}(2):\dots:M_{I_1}(-3) = 1:2:3:4:3:2:1$, and $M_{I_2}(9):M_{I_2}(8):\dots:M_{I_2}(-9) = 1:6:21:56:120:216:336:456:546:580:546:\dots:6:1$. The position of H and the relative intensity ratios of 7×19 or 133 hyperfine lines can be calculated in the manner similar to the case of the $\langle 110 \rangle$ direction. As a result, 133 hyperfine lines are segregated into 25 groups and the separation of each line in each group is $2.67b'$ G.

Every observed spectrum in Fig. 1 has the hyperfine structure with more than 20 peaks and the resolution of them for the $\langle 110 \rangle$ and for the $\langle 111 \rangle$

direction is poorer than that for the $\langle 100 \rangle$ direction. In addition, the spectrum in the $\langle 111 \rangle$ direction is slightly less resolved in comparison with that in the $\langle 110 \rangle$ direction. These facts seem to reflect that the separation of each line in each group is $2b'$ G for the $\langle 110 \rangle$ and $2.67b'$ G for the $\langle 111 \rangle$ direction. With respect to the resolution of the spectra and the relative intensity ratios of hyperfine lines, the observed spectra are in good agreement with the calculated results. Thus, the features of the characteristic spectra for reactor-irradiated Li₂O single crystals can be reasonably interpreted in terms of the F^+ center.

In the calculated results, the separations of 25 lines (for the $\langle 100 \rangle$ direction) or the most intense lines in 25 groups of hyperfine lines (for the $\langle 110 \rangle$ and the $\langle 111 \rangle$ direction) are a' G for the $\langle 100 \rangle$ and for the $\langle 110 \rangle$ direction and $(a' - 0.67b')$ G for the $\langle 111 \rangle$ direction in most cases. From the experimental results, the separation of each peak is found to be 9.5 ± 0.2 G for the $\langle 100 \rangle$ and 9.2 ± 0.2 G for the $\langle 111 \rangle$ directions, respectively. Consequently, a' and b' are determined to be 9.5 ± 0.2 and 0.5 ± 0.4 G, respectively. These values of a' and b' suggest that the hyperfine interaction of the F^+ center in Li₂O is almost isotropic (i.e., Fermi contact) and the anisotropic interaction (dipole-dipole interaction) is small.

Furthermore, the isotopic constant is related to the trapped electron density on the surrounding ^7Li nuclei for the F^+ center by,

$$a' = \frac{8\pi}{3} \frac{\mu_N}{I} |\psi_F(\text{Li})|^2, \quad (6)$$

where μ_N is the magnetic moment of ^7Li nucleus and $|\psi_F(\text{Li})|^2$ is the trapped electron density on the surrounding ^7Li nuclei. From the experimental value of a' , $|\psi_F(\text{Li})|^2$ was determined to be $0.10 \times 10^{30} \text{ m}^{-3}$. Since $|\psi_{2s}(0)|^2$ of a free Li atom is assumed to be about $1.12 \times 10^{30} \text{ m}^{-3}$,⁸ the trapped electron on the surrounding ^7Li nuclei has a density of about 9% of that of free Li atoms. The value obtained above is approximately equal to that determined for the F^+ center in neutron-irradiated Li₂O pressed powder.⁴

Spin concentration of the F^+ centers was determined for the specimens irradiated to different neutron fluences by comparing the intensity of the spectra with that of diphenylpicrylhydrazyl (DPPH) in chloroform of known concentration and are shown in Fig. 3. The concentration was 1.8×10^{23} , 3.7×10^{23} , and 2.8×10^{24} F^+ centers per m^3 for the specimens irradiated to 4.2×10^{20} , 4.5×10^{21} , and 1.7×10^{23} thermal neutrons per m^2 , respectively. The inducing efficiency of the F^+ centers decreases gradually with the neutron fluences. In the study of optical absorption³ in Li₂O single crystals irradiated to above 4×10^{20} thermal neutrons per m^2 , some absorption bands similar to aggregate centers were observed and they grew with neutron fluences. This suggests the conversion of the F^+ centers to aggregate centers during

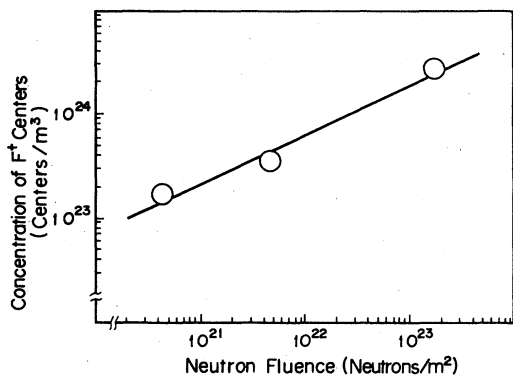


FIG. 3. A relationship between the concentration of the F^+ center and neutron fluences.

irradiation, which cannot be detected by ESR because of lack of unpaired electrons. Furthermore, some of the F^+ centers might be annihilated by migration of interstitials, since it was easy for interstitials to move at ambient temperatures under irradiation.

In the sintered pellets and pressed powder of Li_2O irradiated to the order of 10^{23} thermal neutrons per m^2 , a narrow and isotropic ESR line was observed in addition to those of the F^+ centers. The isotropic spectrum was attributed to colloidal Li metal centers.^{4,5} In contrast with the above cases, only the F^+ center was detected in the single crystals irradiated to the order of 10^{23} thermal neutrons per m^2 . This suggests that grain boundaries of the sintered pellets and surfaces of the pressed powder play an important role in precipitation of the colloidal Li metals.

B. Annealing behavior of the F^+ center

The annealing behavior of the F^+ centers was investigated by the isochronal annealing method as well as by the isothermal annealing method. In the isochronal annealing experiments, Li_2O single crystals irradiated to 3.8×10^{20} , 4.5×10^{21} , and 1.7×10^{23} thermal neutrons per m^2 were heated to 650 K for 1800 sec at intervals of about 50 K. The ESR spectra of the specimens were observed at room temperature in the $\langle 111 \rangle$ direction of the specimen immediately after each annealing, and each intensity was determined by the area of the spectrum. The intensity normalized to that before annealing is shown as a function of annealing temperature in Fig. 4. For the specimens irradiated to 4.5×10^{21} and 1.7×10^{23} thermal neutrons per m^2 , a complete disappearance of the F^+ center at about 630 K followed after an initial decrease in the intensity at about 420 K and a remarkable decrease between 520 and 600 K. On the other

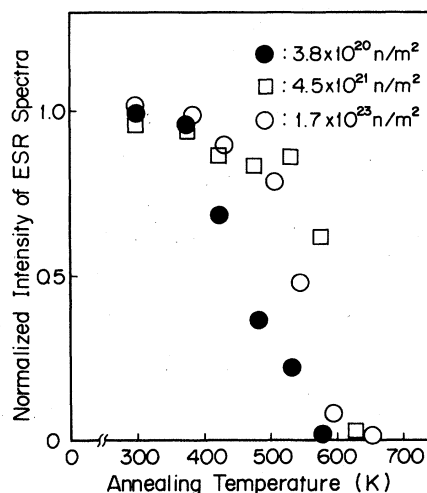


FIG. 4. The behavior of the F^+ center during isochronal annealing experiments for specimens irradiated to various neutron fluences.

hand, for the specimen irradiated to 3.8×10^{20} thermal neutrons per m^2 , a complete disappearance at 580 K followed after the considerable decrease at 420 K.

The difference of temperature initiating the recovery of the F^+ centers in neutron fluences seems to arise from the difference in the amount and distribution of the F^+ centers rather than that in the specimens used. In the ESR study of sintered Li_2O pellets⁵ and the optical absorption study of Li_2O single crystals and sintered pellets,³ similar behavior of recovery of the F^+ centers during isochronal annealing was observed.

Isothermal annealing experiments were carried out at 530, 580, and 630 K for the specimens irradiated to 4.1×10^{21} or 5.3×10^{21} thermal neutrons per m^2 . The specimens were kept at the annealing temperature for various periods and then the ESR spectra were observed at room temperature. Figure 5 shows intensity of ESR spectra normalized to that before annealing versus annealing times for three annealing temperatures.

From these isothermal annealing curves, the activation energy for recovery of the F^+ centers, E_r , was obtained. Decrease of concentration of the F^+ centers, C , is assumed to be expressed by

$$\frac{dC}{dt} = -f \exp\left(-\frac{E_r}{kT}\right), \quad (7)$$

where t is the time, f is the function related to only C , and other symbols have the usual meanings. Equation (7) is integrated between as-irradiated concentration C_0 and a concentration C during anneal-

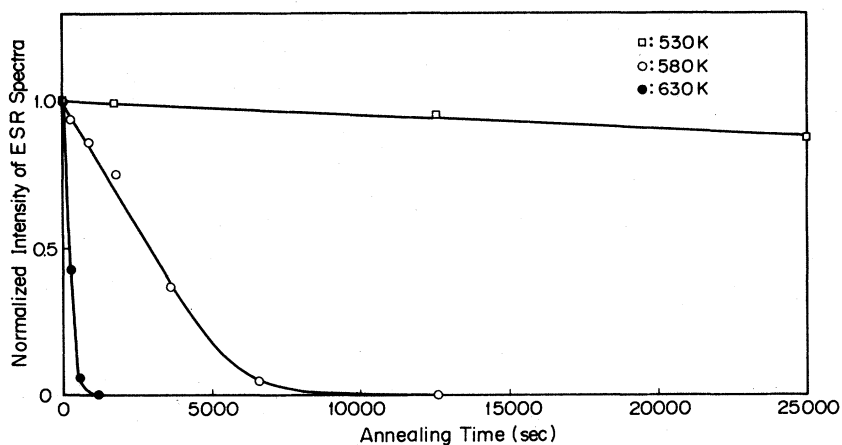


FIG. 5. The behavior of the F^+ center during isothermal annealing experiments at various temperatures for specimens irradiated to the order of 10^{21} thermal neutrons per m^2 .

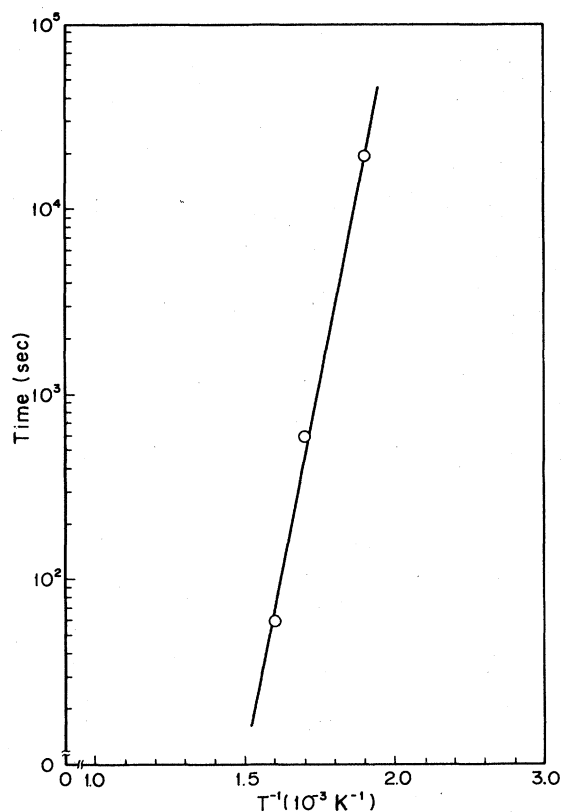


FIG. 6. The relationship between the annealing time and the inverse of annealing temperature in the isothermal annealing experiments.

ing, and the following equation is obtained:

$$-\int_{c_0}^c \frac{dC}{f} = \text{const} = t \exp\left[-\frac{E_r}{kT}\right], \quad (8)$$

i.e.,

$$\log_{10} t = \text{const} + \frac{E_r}{2.303k} \left(\frac{1}{T}\right). \quad (8')$$

In Fig. 6, the annealing times t are shown versus the inverse of annealing temperature $1/T$. According to Eq. (8'), the activation energy for the recovery of the F^+ centers in Li_2O is determined to be about 135 kJ/mol (1.4 eV).

ACKNOWLEDGMENTS

The authors wish to express their thanks to Dr. S. Mori, Dr. S. Nomura, Dr. J. Shimokawa, Dr. Y. Obata, Dr. R. Nagasaki, Dr. T. Kikuchi, and Dr. K. Sako for their interest in this work. The authors would like to thank Professor Dr. T. Kiriara of Nagoya University for his kind guidance on this work. We also thank Dr. Y. Itoh and Dr. Y. Kazumata for making ESR spectrometers available and for their helpful discussions. One of the authors is grateful to JAERI for financial support as a research student.

*On leave of absence from Nagoya University, as a Research Student, 1980.

- ¹K. Sako, M. Ohta, Y. Seki, H. Yamato, T. Hiraoka, T. Tanaka, N. Asami, and S. Mori (unpublished).
- ²E. M. Larsen, S. I. Abdel-Khalik, and M. S. Ortman, Nucl. Technol. 41, 12 (1978).
- ³K. Uchida, K. Noda, T. Tanifuji, S. Nasu, T. Kirihara, and A. Kikuchi, Phys. Status Solidi A 58, 557 (1980).
- ⁴Y. Ueda, Y. Kasumata, and M. Nishi, Jpn. J. Appl. Phys. 16, 1743 (1977).
- ⁵K. Noda, K. Uchida, T. Tanifuji, and S. Nasu, J. Nucl. Mater. 91, 234 (1980).
- ⁶I. Shindo, S. Kimura, K. Noda, T. Kurasawa, and S. Nasu, J. Nucl. Mater. 79, 418 (1979).
- ⁷R. Kaplan and P. J. Bray, Phys. Rev. 129, 1919 (1963).
- ⁸J. A. McMillan and T. Halpern (unpublished).